# Pressure-induced localisation of the hydrogen-bond network in KOH-VI

Andreas Hermann, Malcolm Guthrie, Richard J. Nelmes, and John S. Loveday

Citation: The Journal of Chemical Physics **143**, 244706 (2015); doi: 10.1063/1.4938260
View online: http://dx.doi.org/10.1063/1.4938260
View Table of Contents: http://scitation.aip.org/content/aip/journal/jcp/143/24?ver=pdfcov
Published by the AIP Publishing





# Pressure-induced localisation of the hydrogen-bond network in KOH-VI

Andreas Hermann,[1,a)] Malcolm Guthrie,[1,2] Richard J. Nelmes,[1] and John S. Loveday[1]
[1]*Centre for Science at Extreme Conditions and SUPA, School of Physics and Astronomy, The University of Edinburgh, Edinburgh EH9 3JZ, United Kingdom*
[2]*European Spallation Source AB, P.O. Box 176, SE-22100 Lund, Sweden*

(Received 25 September 2015; accepted 27 November 2015; published online 29 December 2015)

Using a combination of *ab initio* crystal structure prediction and neutron diffraction techniques, we have solved the full structure of KOH-VI at 7 GPa. Rather than being orthorhombic and proton-ordered as had previously be proposed, we find that this high-pressure phase of potassium hydroxide is tetragonal (space group $I4/mmm$) and proton disordered. It has an unusual hydrogen bond topology, where the hydroxyl groups form isolated hydrogen-bonded square planar $(OH)_4$ units. This structure is stable above 6.5 GPa and, despite being macroscopically proton-disordered, local ice rules enforce microscopic order of the hydrogen bonds. We suggest the use of this novel type of structure to study concerted proton tunneling in the solid state, while the topology of the hydrogen bond network could conceivably be exploited in data storage applications based solely on the manipulations of hydrogen bonds. The unusual localisation of the hydrogen bond network under applied pressure is found to be favored by a more compact packing of the constituents in a distorted cesium chloride structure. © *2015 AIP Publishing LLC.* [http://dx.doi.org/10.1063/1.4938260]

## I. INTRODUCTION

Alkali hydroxides MOH, with alkali metal M ranging from lithium to cesium, are intriguing compounds. They are partly ionic (in an idealised world, they are $M^+(OH)^-$) and partly hydrogen-bonded solids, as the hydroxyl groups $OH^-$ can (and do) form hydrogen-bonded networks. The nature of those hydrogen bond networks, and their manipulation by changes in temperature or external pressure, has been the subject of numerous experimental and computational studies.[1–12] The response of the hydrogen bond network structure to increasing density in these systems is of particular interest. For instance, there is considerable evidence that the $OH^-$ anion behaves differently from molecular OH groups, but the origin of this phenomenon is not fully resolved.

Alkali hydroxides also serve as arguably the simplest model systems for hydrous minerals. Those are complex phases within the $MgO—SiO_2—H_2O$ and $Al_2O_3—SiO_2—H_2O$ systems and are assumed to be important carriers of water into Earth's mantle.[13–15] Current estimates suggest that Earth's mantle contains three times the amount of water in its oceans.[16,17] This water is often present in the form of hydroxyl groups[18] and also related to uptake in nominally anhydrous minerals such as olivine and its high-pressure phases wadsleyite and ringwoodite. The presence of water in these minerals can drastically affect their physical properties, such as mechanical strength, elasticity, and internal ionic diffusion rates,[19,20] and the topologies of hydrogen-bond networks are expected to play a major role in determining those parameters. Hydrous phases that are stable at high pressures are often not recorded in natural samples, and hence computational and laboratory investigations into hydrogen-bonded networks under compression are highly relevant. Alkali hydroxides have the additional advantage that, from lithium to cesium, a wide range of cation sizes can be introduced, and their influence on the structural choices of the hydrogen bond networks be examined.

Here, as part of an investigation into systematic trends observed in the alkali hydroxides under compression, we examine the high-pressure phase transition exhibited by potassium hydroxide, KOH (or its deuterated analogue KOD), at around P = 6.5 GPa. Our structural assignment, based on neutron powder diffraction experiments and first-principles electronic structure calculations, suggests that the high-pressure phase of potassium hydroxide features localised square planar, proton-disordered, and hydrogen-bonded $(OH)_4$ units—a network topology not seen before in any alkali hydroxide or similar compound. Localised hydrogen-bonded entities, usually water, have been found before in relatively complex host matrices.[21–23] Other low-dimensional hydrogen-bonded water arrangements, like chains and helices, have been found in bulk or surface studies.[24,25] The creation of such a configuration in potassium hydroxide is arguably much simpler and, as we suggest below, should allow for the targeted manipulation of the localised hydrogen-bonded units, for instance, to study the dynamics of correlated tunnelling in hydrogen bonds.[26] The hydrogen-bond network in each unit can take up one of two states, with clockwise or anti-clockwise directions of the hydrogen bonds. This binary degree of freedom could conceivably be used as a new type of data storage medium, based solely on the orientation and manipulation of hydrogen bonds. In principle, an areal storage density of the order of 1 Pbit/in.$^2$ could be realised in a thin film of such a material, much surpassing storage densities available in electronic flash memory or optical storage media.[27–29]

a)a.hermann@ed.ac.uk

 

## II. METHODS

### A. Diffraction studies

Samples of KOD[30] were studied using the Paris-Edinburgh cell[31] at the PEARL high-pressure beam line at the ISIS pulsed neutron source. Samples were produced by dehydration of KOD solutions obtained from Sigma-Aldrich at 200 °C in a vacuum oven. The use of vacuum of better than $10^{-3}$ bars was found to be important to ensure full dehydration and to avoid the contamination of the sample with KOD hydrate. The resulting solid KOD was powdered and loaded under fluorinert into the pressure cell. The sample was compressed by increasing the applied load and the change in the structure was followed by measurement of the diffraction pattern. The loaded cell was placed on the beam line and neutron diffraction data were collected in ~1 GPa steps up to and beyond the transition at ~6.5 GPa.[7] Data collection times varied from ~1 h runs for the purposes of phase identification to 6-8 h runs for precise refinement of the structural parameters. The data collected were corrected for the effects of wavelength dependent attenuation of the neutron beam by the tungsten carbide anvils and other pressure cell materials[32] and analysed by Rietveld profile refinement using the GSAS package.[33] The pressure was estimated by comparison of the measured lattice parameters with those published by Otto and Holzapfel for KOH.[7]

### B. First-principles calculations

To screen for potential structures of the high-pressure phase of potassium hydroxide, we performed a ground-state crystal structure search with four formula units per unit cell at P = 10 GPa, which corresponds to the unit cell size that can be deduced from x-ray data[7] and is well above the experimental phase transition pressure. We used the evolutionary algorithm approach as implemented in the XtalOpt package[34] in conjunction with density functional total-energy calculations using the VASP package.[35,36] Candidate structures were then optimised across the entire pressure range from P = 1 atm to P = 200 GPa (mostly to study hydrogen-bond symmetrization, see text below; note that other phases might emerge as more stable at high pressures). Density functional calculations used the PBE exchange-correlation functional[37] to describe the electron-electron interaction and regular k-point grids of linear density 20/Å$^{-1}$. The projector augmented wave method (PAW) was used to model the electron-ion interaction, using K($3p^6 4s^1$)O($2s^2 2p^6$)H($1s^1$) valence PAW datasets with cutoff radii K(3.0)O(1.52)H(1.1) $a_B$. A plane wave energy cutoff energy of $E_c$ = 600 eV was employed. All structures were optimised until remaining force components were less than 1 meV/Å. Nudged-elastic band calculations[38] were performed using 24 images. Zone-center phonon frequencies were obtained using the finite difference method.

## III. POTASSIUM AND OTHER ALKALI HYDROXIDES

At $P = 1$ atm and room temperature, KOH and KOD form a monoclinic, layered structure with space group $P2_1/m$,[4] see left hand side of Figure 1. The oxygen-potassium sub-lattice actually resembles a sodium chloride structure (see the supplementary material,[39] for a visualization), attesting to the ionic character of the material, but the orientations of the OH groups lead to monoclinic distortions and the bilayer arrangement suggested in Figure 1. The proton/deuteron sites are half-occupied, and their location corresponds to a small rotation of the OH groups. In either site, an OH group can form a hydrogen bond to a OH group in the adjacent bilayer. Overall, this phase of KOH/KOD thus has one-dimensional proton-disordered hydrogen-bonded chains connecting the bilayers. The same feature is found in all alkali hydroxides (except LiOH(D)) at ambient conditions. In KOH, this phase is labelled KOH-II, as per notation by Krobok and Holzapfel.[6] At high temperatures (above $T$ = 523 K for KOD[4]), the hydrogen bonds break, the hydroxyl groups become quasi-free rotors, and the overall structure is cubic, of the sodium chloride type; this is the KOH-I phase.

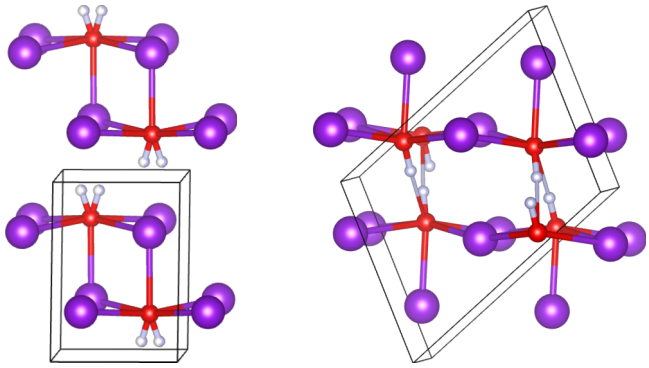

FIG. 1. Experimentally determined structures of KOD at atmospheric pressure. Left: room-temperature $P2_1/m$-KOD-II; right: low-temperature $P2_1/n$-KOD-IVa. Purple, red and white spheres denote K, O, and D atoms, respectively. Note half-occupancy of deuterium sites in $P2_1/m$-KOD-II (KOD-II also transforms to KOD-IVa on compression, at $P = 0.7$ GPa at room temperature).

At low temperatures ($T$ = 233 K for KOH and $T$ = 257 K for KOD), the material undergoes a proton-ordering transition,[3,4] leading to a monoclinic structure of $P2_1/n$ symmetry, as shown on the right hand side of Figure 1. In that low-temperature phase, labelled KOH-IVa, polarisations of adjacent hydrogen-bonded chains are opposing each other, leading to an overall antiferroelectric arrangement. All other alkali hydroxides (except for LiOH(D), and NaOH) exhibit similar proton-ordering within the $OH^-$ chains upon cooling, with overall antiferroelectric order in NaOD and CsOH(D) and ferroelectric order in RbOH(D).

It has been argued[7] that compression at room temperature could induce the same or similar phase transitions in those compounds, and phase transitions at moderate pressures (P < 1 GPa = 10 kbar) have indeed been found in all alkali hydroxides and deuteroxides.[5–8] For potassium, rubidium, and cesium hydroxides, these pressure-induced transitions resulted in the respective low-temperature ambient-pressure phases, with $P2_1/m$-KOH-II transforming to $P2_1/n$-KOH-IVa at $P = 0.7$ GPa at room temperature.[6] Further compression results in the formation of denser phases that are presumed to be non-layered.[7] KOH transforms at $P$ = 6.5 GPa to the KOH-VI phase, the structure of which has been uncertain.

For NaOH, the structure of the high-pressure phase (NaOH-V) has been shown by a combination of x-ray[40] and neutron powder diffraction[8] to be non-layered with a pseudo-NiAs arrangement of the heavy atoms and an extended two-dimensional hydrogen bond network which includes a bifurcated hydrogen bond.[8] Otto and Holzapfel suggested that the high-pressure phases of potassium and rubidium hydroxide (KOH-VI and RbOH-VI) have an orthorhombic "anti-NaOH" structure,[7] based on the similarities between the unit cell dimensions of these phases and those of NaOH-V. What this structure is was not made clear, but we take it to mean that the anion and cation sites in the potassium and rubidium hydroxide structures are swapped with respect to their arrangement in sodium hydroxide-V. Since Otto and Holzapfel measured only energy dispersive x-ray diffraction (EDX), no information could be obtained on the full structures (atomic fractional co-ordinates) and hydrogen-bond networks of either potassium hydroxide-VI or rubidium hydroxide-VI. Previous work by the same group found significant hardening of the OH stretch mode across the phase transition, possibly indicating weaker hydrogen bonding in the high-pressure phases.[6]

## IV. RESULTS

### A. Crystal structure prediction

The relative ground state enthalpies of relevant phases that emerged from our structure searches or that are known structure types of the alkali hydroxides, are shown in Figure 2. Our calculations confirm the low-temperature $P2_1/n$-KOH-IVa phase as the most stable phase for KOH at atmospheric and low pressures.[41] At P = 9 GPa in our calculations, two

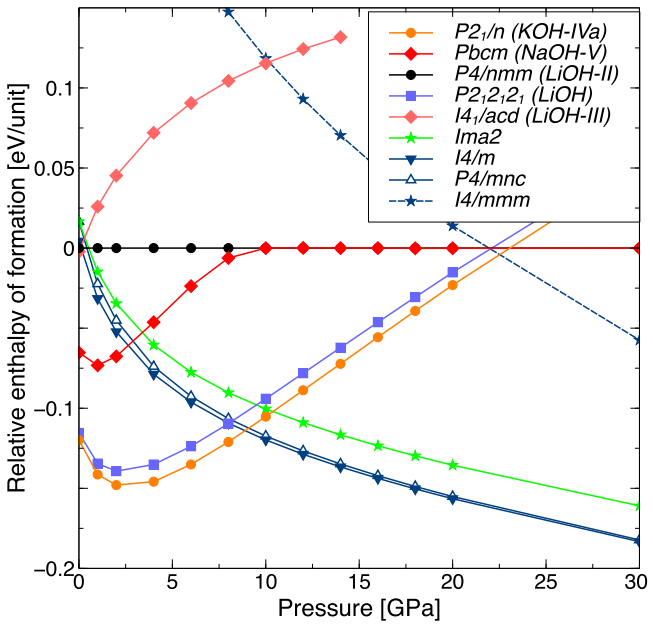


FIG. 2. Relative ground state enthalpies of formation of various KOH phases, classified by their space group symmetries and based on known alkali hydroxide structure types (listed in brackets) or results from our crystal structure search at $P = 10$ GPa. Note the $I4/mmm$ phase here is not the same as the one shown in Figure 4 (see text in Section IV B).

tetragonal structures of $I4/m$ and $P4/mnc$ symmetry emerge as more stable than the $P2_1/n$ phase. These two structures, shown in Figure 3, are tetragonal, whereas the NaOH-V structure type is orthorhombic (space group *Pbcm*). However, in the EDX experiments on potassium hydroxide-VI, the assigned *Pbcm* orthorhombic cell has a *b* lattice parameter that is within 0.5% of twice the *a* lattice parameter.[7] An orthorhombic splitting that small cannot be resolved within the resolution of the EDX experiment by Otto and Holzapfel (or the neutron data presented here) so that it is not possible to rule out a tetragonal structure on the basis of the positions of the Bragg peaks alone. However, the DFT calculations show that the *Pbcm* NaOH-V structure is not energetically competitive for potassium hydroxide.

The energetically competitive phases are locally very similar. They feature localised potassium ions and covalently bound hydroxyl groups; the latter are connected via OH···O hydrogen bonds. The substantial energetic differences seen in Figure 2 stem from the global arrangements of these building blocks, as will be discussed below. As a consequence, however, we can neglect zero-point contributions to the relative enthalpies, which (because of their chemical similarity) should be very similar across all competitive phases.

### B. Structure solution

The transition sequence observed under pressure corresponded closely to that reported by Otto and Holzapfel, with a transition from the $P2_1/m$ phase to the $P2_1/n$ phase at $P \approx 1$ GPa and then to another phase with a different structure at $P \approx 6.5$ GPa. This transition sequence was observed in more than three loadings of the Paris-Edinburgh cell. A representative example of the high-pressure diffraction pattern is shown in Figure 4. Analysis of our data failed to find an acceptably plausible fit with either the "anti-NaOH" structure proposed by Otto and Holzapfel[7] or, in fact, any other structure in which the oxygen and potassium atoms follow *Pbcm* space group symmetry. On that basis, we did not consider the *Pbcm* symmetry any further.

In light of the calculation results, the systematic absences of the diffraction data were examined. $P4/mnc$ has further additional reflections when compared to $I4/m$. The positions of five of these additional reflections were free from overlap, yet none were observed. The diffraction data thus showed no visible breaking of body-centred tetragonal symmetry and thus suggest that $P4/mnc$ is inconsistent with the data. However, considering the closeness in enthalpy of the two structures (see below), a fit to the data was first needed to check that $P4/mnc$ puts detectable intensity into those five unobserved reflections.

Refinements with both tetragonal structures were stable and gave weighted profile R-factors, $R_{wp}$, of 5.06% for $P4/mnc$ and 4.61% for $I4/m$, each with 34 variables. The $I4/m$ structure thus gave a significantly better fit, and inspection of the fit with the $P4/mnc$ model showed small but visible calculated intensity for the five reflections whose positions are observable that distinguish $P4/mnc$ from $I4/m$ (see above). This calculated intensity was not present in the observed data. On these grounds, the $P4/mnc$ model was ruled out. The fit

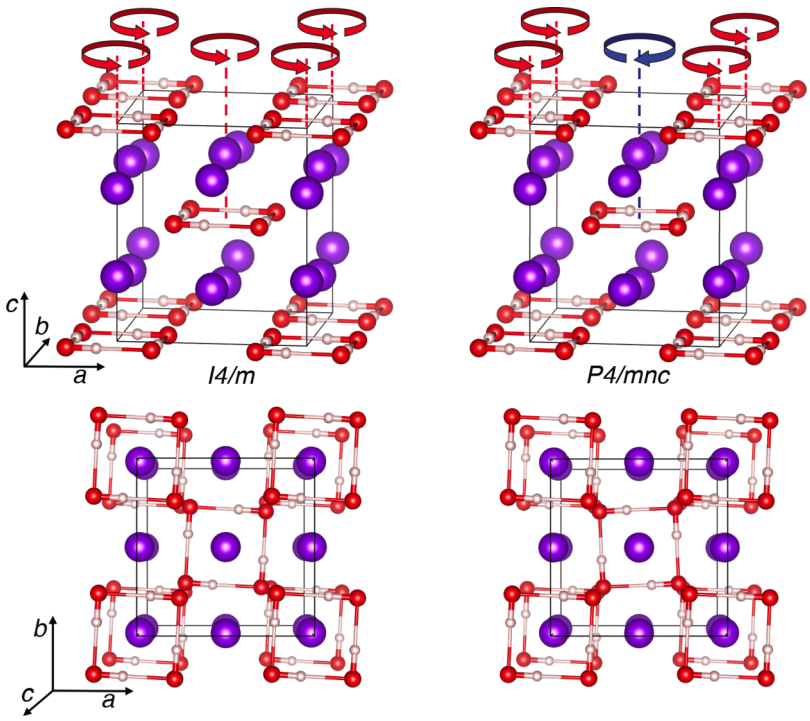


FIG. 3. Predicted $I4/m$ and $P4/mnc$ crystal structures of potassium hydroxide-VI, at P = 10 GPa, in side view with orientations of hydrogen bond networks indicated (upper panel), and top view (lower panel). Purple, red and white spheres denote K, O, and H atoms, respectively. Thick (thin) lines denote covalent (hydrogen) bonds.

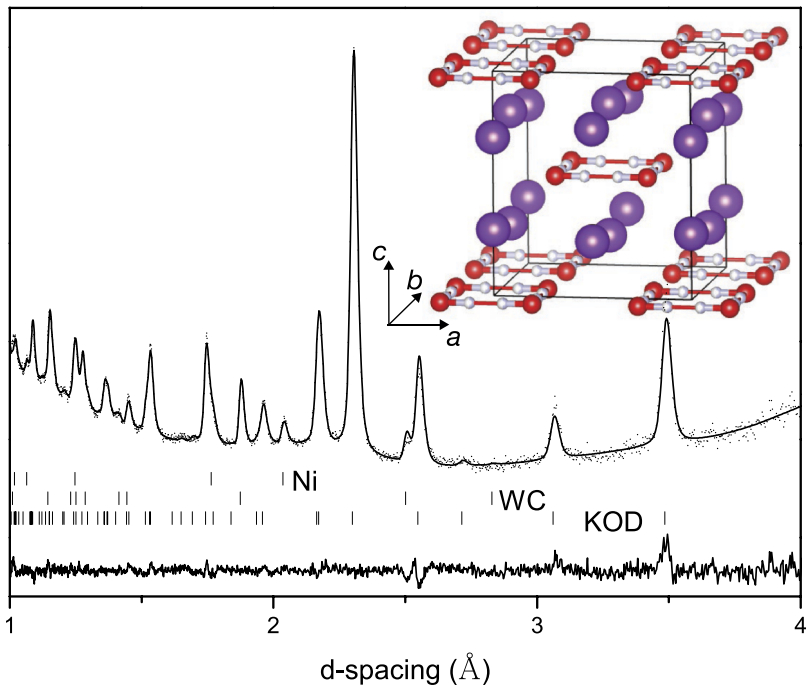


FIG. 4. A Rietveld profile refinement of data collected at room temperature and 7.0 GPa from KOD. The points show the data and the line through the points is the fit obtained using the proton-disordered $I4/mmm$ structural model shown in the inset and described in the text. The vertical marks show the expected positions of the reflections of KOD (bottom), tungsten carbide (middle), and nickel (top). The latter two components are the residual diffraction signal from the anvils of the pressure cell.

to the $I4/m$ model, though plausible, was still poorer than expected given the quality of the data, and it was found that, when refined, the occupancy of the ordered, off-centre D(H) sites shown in Table I and Figure 3 (left) moved to a value of 0.47(5) with a significant improvement in fit. As a result, a model was adopted in which the protons are disordered over two sites with 50% occupancy located symmetrically either side of the hydrogen-bond centre, at the co-ordinates given in Table I. When the protons in the $I4/m$ and $P4/mnc$ structures as shown in Figure 3 are disordered in this way, the resultant disordered hydrogen bonds in *both* structures refine to the $I4/mmm$ structure shown in the inset to Figure 4. This model produced the good fit shown in Figure 4 with a $R_{wp}$ of 2.75% for 32 variables with the crystal structure data given in Table I. Refinements of data collected in this phase from three other samples gave results that were within error the same as those tabulated. Given the significant improvement in fit for fewer variable parameters over the proton-ordered structure, the excellent fit to the data, and the physically reasonable bond lengths and angles, it is clear that the true structure is macroscopically proton disordered. The solution also illustrates valuable complementarity between diffraction studies and electronic structure calculations. The calculations are only able to probe ordered configurations

TABLE I. Crystal structures of potassium hydroxide-VI from structure refinement ($I4/mmm$) and our ground state calculations ($I4/m$ and $P4/mnc$), all at P = 7.0 GPa.

| Phase | a, c (Å) | Atomic positions |
|---|---|---|
| $I4/mmm$ (Exp.) | 6.1202, 6.9713 | $K_1$(0, 1/2, 1/4)<br>$K_2$(0,0,0.2907(9))<br>O(−0.2348(4),0.2348(4), 0)<br>D(0.0894(5),0.2273(6),0) |
| $I4/m$ (DFT) | 6.217, 7.149 | $K_1$(0, 1/2, 1/4)<br>$K_2$(0, 0, 0.297)<br>O(−0.211, 0.243, 0)<br>H(0.085, 0.225, 0) |
| $P4/mnc$ (DFT) | 6.211, 7.154 | $K_1$(0, 1/2, 1/4)<br>$K_2$(0, 0, 0.297)<br>O(−0.214, 0.240, 0)<br>H(0.081, 0.225, 0) |

and hence cannot predict disorder, while the latter can be identified from the diffraction data. In that context, note that the $I4/mmm$ phase included in Figure 2 is not the same as the proton-disordered phase discussed above. Instead, it represents a proton-ordered phase with all protons positioned at the mid-points between oxygen atoms within the $(OH)_4$ units (see the supplementary material for structural details).[39] Such a symmetric hydrogen bond is similar to the proton arrangement in the high-pressure phase of ice, ice-X, and ordered $I4/mmm$ thus represents the high-pressure limit of all of the $I4/m$, $P4/mnc$, and the disordered $I4/mmm$ structures. This phase is relevant only at very high pressures: in the ground state, we find hydrogen bond symmetrization in KOH to occur at $P$ = 160 GPa (the transition to a new high-pressure phase, KOH-VII); in experiment, this pressure might be substantially lower due to the quantum nature of the proton.[42,43]

We can compare calculated IR/Raman frequencies for the KOH-IVa and the suggested KOH-VI phases with experimental data on the OH stretch modes from Krobok and Holzapfel,[6] as shown in Figure 5 as function of pressure. To acknowledge the strong anharmonicity of the OH stretch, we have shifted the frequency axis of the calculations by 80 $cm^{-1}$. In the low-pressure KOH-IVa phase, our calculations reproduce very well the splitting between the different stretch modes and the rapid frequency decrease as pressure is increased. This indicates significant weakening of the OH covalent bond, as hydrogen bonds are strengthened. For the high-pressure KOH-VI phase, our calculations (which assume the $I4/m$ structure) reproduce the increase in OH stretch frequencies by 50-100 $cm^{-1}$ at the phase transition, followed by rapid decrease. This frequency increase in KOH-VI would indicate a weaker hydrogen bond network, at the same pressure, than in KOH-IVa, and it is conceivable that the localised $(OH)_4$ units are less strongly hydrogen bonded than the extended chains seen in $P2_1/n$-KOH-IVa (see below for more details). Note that in the experimental data, the highest Raman active mode of KOH-IVa seemingly extends up to 15 GPa, far above the transition pressure. Our calculations show that this is in fact a KOH-VI stretch mode

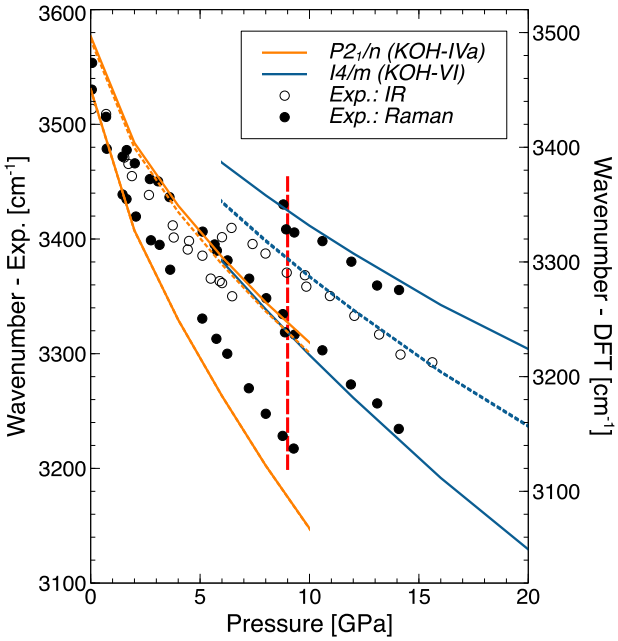


FIG. 5. Calculated OH vibron frequencies for $P2_1/n$-KOH and $I4/m$-KOH as function of pressure, compared to IR/Raman peak positions taken from experiment (Ref. 6). Filled/open symbols denote experimental Raman/IR peak positions, and solid/dashed lines denote calculated Raman/IR-active modes. The vertical red dashed line indicates the transition pressure as calculated from DFT.

that coincides across the entire pressure range with the highest stretch mode of KOH-IVa.

## V. DISCUSSION

Let us consider the nature of the proposed structure, and how the disordered and two ordered forms are related. The oxygen and potassium atoms in the $I4/m$ and $P4/mnc$ ordered structures form a distorted cesium chloride-like arrangement in an $(a/2, a/2, c/2)$ "unit cell" (see Figure 3 and also the supplementary material).[39] This is a reasonable choice for a compound with significant ionic bonding, yet markedly different from the NaOH-V phase, which is based on the nickel arsenide structure. In KOH, each oxygen is displaced along the $a$ and $b$ axes from the centre of the surrounding group of eight potassiums to form localised hydrogen-bonded square planar $(OH)_4$ units, in which all the OH bonds lie in the same $ab$ plane as the oxygens. There are two such $(OH)_4$ units in the unit cells of both structures. The two structures differ in the relative orientation of the hydrogen-bond network in those two $(OH)_4$ units: in $I4/m$, all units are oriented the same way (say, anticlockwise, as shown in Figure 3 when looking down the $c$ axis), whereas, in $P4/mnc$, units in adjacent $ab$ planes are oriented in opposite senses (clockwise and anticlockwise). This difference is pointed out schematically by arrows in Figure 3. The ground state enthalpy difference between the structures is small: at P = 7 GPa, $I4/m$ is more stable than $P4/mnc$ by 3 meV/formula unit. This suggests that the formation of ordered domains of like-oriented $(OH)_4$ units is energetically favourable. However, the energy cost to invert the hydrogen bond network of a single $(OH)_4$ unit is

also small so that, at room temperature, the orientation of each $(OH)_4$ square could be random, leading to an overall structure that is proton disordered on the lengthscale (mm) and time scale (hours) of the diffraction measurement. This is consistent with our structural refinement, which favoured the $I4/mmm$ structure of Table I. However, it seems highly likely that locally this structure will obey a hydroxyl equivalent of the ice rules[44] where each hydroxyl group donates and accepts one H-bond. Such a rule applies to the low-temperature ordered structures of potassium, rubidium, and cesium hydroxide. As a consequence, in the case of potassium hydroxide-VI, the choice of a single OH orientation within each $(OH)_4$ square is likely to determine the orientation of all other OH groups in the square. Otherwise, energetically costly defects would be introduced, which were estimated by rotating a single OH group in one $(OH)_4$ unit in the $I4/m$ phase, thus creating a pair of Bjerrum defects,[45] at a cost of 1.27 eV/pair at P = 1 atm and 2.58 eV/pair at P = 10 GPa. In other words, the hydrogen-bond network in high-pressure potassium hydroxide is always locally orientationally ordered, but our room-temperature diffraction data are only sensitive to a long-range spatially and temporally averaged structure. At sufficiently low temperature, potassium hydroxide should be ordered globally, most probably in the $I4/m$ structure.

In general, potassium hydroxide represents a curious case: as mentioned earlier, its low-pressure phases KOH-II and KOH-IVa have an *extended* hydrogen bond network, in the form of infinite zig-zag chains of OH groups, whereas its high-pressure phase KOH-VI has a *localised* hydrogen bond network, in the form of well-separated square planar $(OH)_4$ units. Thus, the effect of pressure is to reduce the dimensionality of the H-bonding network from one to zero. This contrasts with conventional behaviour where the effect of pressure would be to increase the dimensionality of a network (this is not restricted to hydrogen bonds): compression pushes chains closer together to form layers, and layers are eventually pushed together to form three-dimensional structures. This is how molecular crystals polymerise (like water,[46,47] nitrogen,[48,49] or carbon dioxide[50]), and how compressed graphite forms three-dimensional carbon allotropes.[51] But pressure can also lead to surprising effects: valence electrons, instead of delocalising in a compressed metal, can localise in cavities between the nuclei and create "electrides;"[52,53] nitrogen is predicted to leave the polymeric state and forms a metallic salt;[54] water ice is predicted to transform from three-dimensional networks to layered structures.[55] In all those cases, pressure changes the relative size of different contributions to the total free energy of the respective material, and relatively "exotic" states of matter actually become more stable than what would be expected by conventional rationale. Here, we see another manifestation of this effect of compression.

We next turn to the question as to what stabilises this peculiar structure of KOH-VI. Comparing the volumes per formula unit of relevant phases, we see that the $I4/m$ and $P4/mnc$ phases are denser than all others, across the entire pressure range (see the supplementary material for more detail[39]) and they are thus increasingly favoured under compression. At the theoretical transition pressure P = 9 GPa, we calculate a volume collapse of $\Delta V/V = 6\%$. However, is it possible that the localisation of the hydrogen bond network in KOH-VI balances this density increase with an energetic cost, perhaps due to strained hydrogen bond angles? To compare the hydrogen bonded sublattices of the low- and high-pressure phases, we calculate the total energies of a single $(OH)_4$ square (taken from the $I4/m$ phase at P = 1 atm) and a single $(OH)_\infty$ chain (taken from the $P2_1/n$ phase at P = 1 atm), both in large unit cells to avoid spurious interactions. Both configurations have very similar energies, with a slight preference (13 meV/OH) for the $(OH)_4$ square arrangement. Given the flexible and local character of the hydrogen bond, it is plausible that both configurations are close in energy. At any rate, there seems to be no large energy penalty to form localised $(OH)_4$ units.

We then probe the ionicity of the competing phases by calculating the partial charges on each atom based on Bader's topological electron density analysis.[56] The partial charge on the potassium cation is a measure of the overall ionicity of the compound, while the partial charge on the proton probes the charge distribution within the hydroxyl group. The analysis confirms that KOH is an ionic solid, with no discernible difference between the low- and high-pressure phases but becomes slightly less ionic under pressure: from P = 1 atm to P = 20 GPa, the partial charge on potassium decreases from +0.82e to +0.77e, for both the $P2_1/n$ and the $I4/m$ phases. To summarise, KOH-VI is first and foremost an ionic solid (with almost ideal charge transfer from $K^+$ to $OH^-$), and its hydrogen bond network energy is very similar to that of KOH-IVa. What stabilises the structure under pressure is the overall more compact packing of the constituents.

The electronic structure of the high-pressure phase also highlights its ionic character. In Figure 6, we compare the calculated electronic density of states (DOSs) of $P2_1/n$-KOH at P = 1 atm with $I4/m$-KOH at P = 10 GPa, and show the electronic band structure of $I4/m$-KOH at P = 10 GPa. Both DOS's are typical for ionic solids, with localised and well separated valence bands and a large band gap. As a consequence of increased overlap upon compression, the valence bands broaden; this is most prominent in the potassium $3p$ states and the oxygen $2p$ states in the highest occupied bands. The lowest unoccupied bands are dominated by potassium $3d$ states. KOH becomes more transparent under pressure — we calculate band gaps of 5.12 eV for the $I4/m$ phase at 10 GPa vs 3.58 eV for $P2_1/n$ at 1 atm. As seen in other molecular crystals with strong partial charge transfers, we find in our calculations that the band gap in potassium hydroxide increases with increasing pressure.[12,57,58] Note that the band gaps obtained from semilocal exchange-correlation functionals are underestimated due to their nondiscontinuity of the exchange-correlation potential[59] but should describe trends of gap opening or closure correctly. More accurate quasiparticle energies and gaps can be obtained by using the $GW$ method, and optical gaps by solving the Bethe-Salpeter equation for correlated electron-hole pairs.[60–63]

In the high-pressure phase of KOH, each localised $(OH)_4$ unit represents a two-state system, with clockwise and anticlockwise orientations of the hydrogen bond network characterising the two states. The regular arrangement of

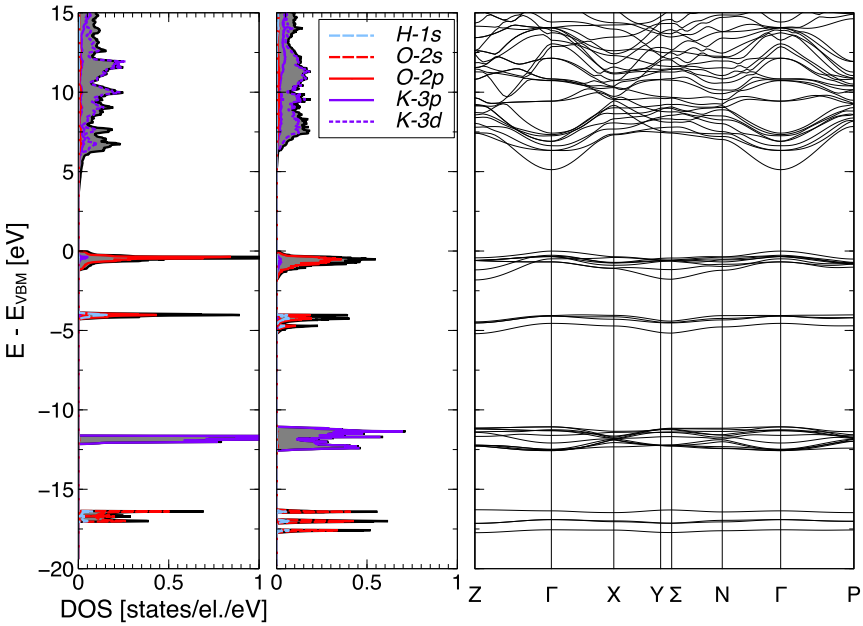


FIG. 6. From left to right: Electronic DOS of $P2_1/n$-KOH at P = 1 atm, of $I4/m$-KOH at P = 10 GPa, and the electronic band structure of $I4/m$-KOH at P = 10 GPa.

the $(OH)_4$ units suggests it could be used, for example, in pump-probe experiments, to study the dynamics of correlated proton motion in hydrogen bond networks. Such correlated tunnelling has been suggested to occur in crystalline phases of ice[26,64] and was observed recently for water tetramers on a NaCl substrate using scanning electron microscopy (SEM).[65] To assess the stability of a given $(OH)_4$ unit, we analyse computationally the barriers of interconversion between the $I4/m$ and $P4/mnc$ structures, which models the switching of the hydrogen bond orientation in one $(OH)_4$ unit. Two possible mechanisms present themselves (see Figure 7 for schematic illustrations): concerted rotation of all OH groups within the $(OH)_4$ unit, or concerted hopping of the four protons along their respective OH $\cdots$ O hydrogen bond. We used the nudged elastic band (NEB) method[38] to find the transition paths and barriers between the two states using both mechanisms, and for pressures from P = 1 atm to P = 20 GPa, well into the stability field of the high-pressure phases. In the second panel of Figure 7, we show the result of these calculations at P = 14 GPa. At that pressure, proton hopping has a lower barrier than OH rotation, with overall transition barriers of 1.71 eV/$(OH)_4$ for OH rotation, and 0.92 eV/$(OH)_4$ for proton hopping. Note that the latter is close to the calculated barriers in the SEM experiments by Meng *et al.*[65] However, their work manipulates a single water tetramer prepared on a surface and benefits from interactions of the SEM tip with the water molecules. Here, a collective reaction within the solid state is proposed.

In the third panel of Figure 7, we show the reaction barriers as a function of pressure. At pressures above P

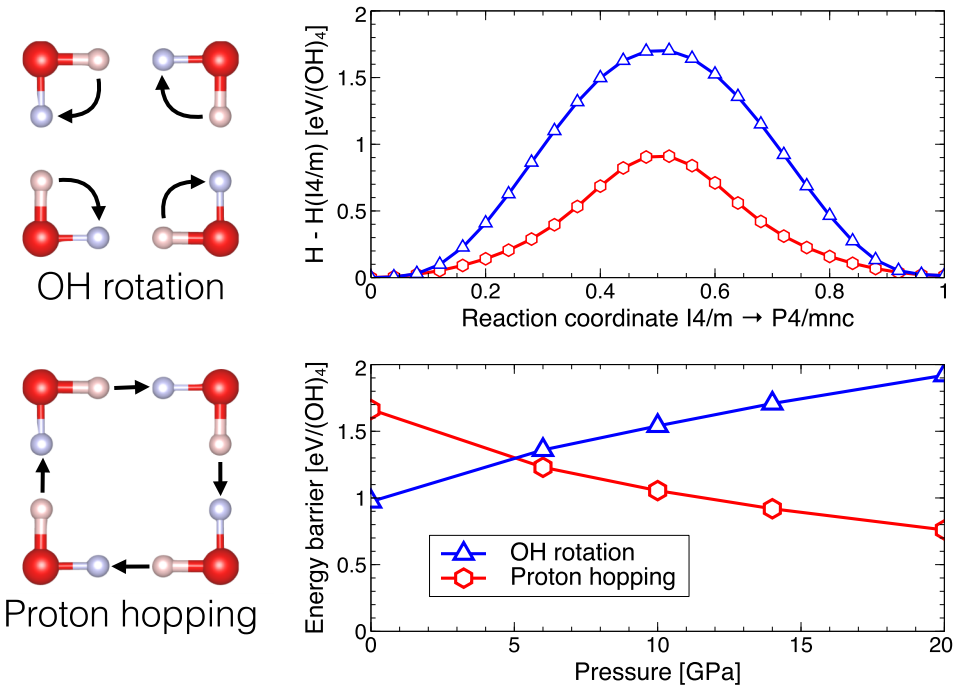


FIG. 7. Transition between the $I4/m$ and $P4/mnc$ potassium hydroxide structures. Left: schematic representation of the "OH rotation" and "proton hopping" mechanisms. Right: transition paths (top, at P = 14 GPa) and barriers (bottom) for both mechanisms.

= 5 GPa, and, in particular, in the region of stability of the $I4/m$ phase at P > 6.5 GPa, proton hopping is the low-barrier mechanism. Under pressure, the covalent OH bond weakens, making it easier to break and to transfer the proton to the neighbouring oxygen atom (which is also closer). At the same time, in the compressed $(OH)_4$ unit, a concerted rotation of the more or less rigid OH groups becomes more difficult. Note that the quantum nature of the proton, which will enhance transition rates, has not been considered here. However, below P = 5 GPa, breaking of the hydrogen bond and rotation of OH groups is energetically preferred over breaking of the covalent OH bond and subsequent hopping of the protons. We would expect this to be the low-barrier process in other materials with such a hydrogen-bond topology if those were prepared at atmospheric pressures.

A switching of the hydrogen bond orientation must couple to vibrational modes that relate to the reaction paths discussed above. At high pressures (around 10 GPa, where $I4/m$ potassium hydroxide is stable), the proton hopping mechanism has the lower barrier and couples to the OH stretch modes. As seen in Figure 5, a mid-IR laser[66] is needed to directly excite the O—H stretching mode around $\nu$ = 100 THz or $\lambda$ = 3 $\mu$m. We note that, in our ground state calculations, $I4/m$ potassium hydroxide remains dynamically stable, and hence energetically metastable, all the way down to atmospheric pressure and is thus potentially recoverable at low temperatures (even though the energetic driving force towards the $P2_1/n$ phase becomes significant, see Figure 2). However, if recovered to P = 1 atm, the low-barrier process of switching between the two states involves OH rotation, and the corresponding phonon modes need slightly lower excitation energies of $\nu$ = 20–27 THz or $\lambda$ = 11–15 $\mu$m, achievable with mid-IR quantum cascade lasers.[67]

## VI. CONCLUSIONS

In conclusion, we present a combined experimental and computational study on the high-pressure phase of potassium hydroxide. We find that, at pressures higher than $P$ = 6.5 GPa, KOH forms a new structure type amongst hydrogen-bonded solids, with discrete $(OH)_4$ units in a metal cation matrix, rather than an extended hydrogen bonded network. In the structure of this KOH-VI phase, the heavy atoms potassium and oxygen are arranged in a distorted cesium chloride structure, with the protons laid out to form localised hydrogen-bonded square planar $(OH)_4$. KOH-VI is predominantly ionic, and benefits from a more compact packing of its constituents than the low-pressure phase KOH-IVa. The structural solution of our room temperature neutron diffraction data shows that the macroscopic proton distribution in the $(OH)_4$ units is disordered. However, hydroxyl "ice rules" suggest that each individual $(OH)_4$ unit is proton-ordered. The structural layout of the $(OH)_4$ units lends itself to studies of correlated proton tunneling, tunable by pressure and based entirely on local hydrogen bond arrangements. Our calculations on transition paths and barriers suggest that those arrangements could be manipulated in the solid state by using infrared laser light. The structural layout of the $(OH)_4$ units leads us to suggest this material as a template for a new kind of digital data storage medium where, ideally, each $(OH)_4$ unit represents one bit of information. KOH-VI itself will not be the material to fulfill this promise — it is neither desirable nor feasible to use a high-pressure phase for such applications, especially with an ordering transition at cryogenic temperatures. However, synthesising the same hydrogen-bond cluster topology at ambient conditions in other simple, inorganic materials would seem to represent a worthwhile avenue to explore.

## ACKNOWLEDGMENTS

We gratefully acknowledge assistance with the experiments from D. J. Francis, W. G. Marshall, and S. Klotz. Computational resources provided by the UK National Supercomputing Service through the UKCP consortium (funded by EPSRC Grant No. EP/K013564/1) and project ID d56 are gratefully acknowledged. The neutron studies were supported by EPSRC through grant funding and by STFC (then CLRC) through access to beam time and other resources. Supplementary research data, in compliance with EPSRC research data policy, can be accessed at http://dx.doi.org/10.7488/ds/392.

[1]D. T. Amm, S. L. Segel, R. D. Heyding, and B. K. Hunter, J. Chem. Phys. **82**, 2529 (1985).
[2]T. J. Bastow, M. M. Elcombe, and C. J. Howard, Solid State Commun. **57**, 339 (1986).
[3]T. J. Bastow, M. M. Elcombe, and C. J. Howard, Solid State Commun. **59**, 257 (1986).
[4]B. Mach, H. Jacobs, and W. Schäfer, Z. Anorg. Allg. Chem. **553**, 187 (1987).
[5]D. M. Adams, A. G. Christy, and J. Haines, J. Phys. Chem. **96**, 8173 (1992).
[6]M. P. Krobok and W. B. Holzapfel, J. Phys.: Condens. Matter **6**, 9789 (1994).
[7]J. W. Otto and W. B. Holzapfel, J. Phys.: Condens. Matter **7**, 5461 (1995).
[8]J. S. Loveday, W. G. Marshall, R. J. Nelmes, S. Klotz, G. Hamel, and J. M. Besson, J. Phys.: Condens. Matter **8**, L597 (1996).
[9]J. M. Kiat, G. Boemare, B. Rieu, and D. Aymes, Solid State Commun. **108**, 241 (1998).
[10]P. W. R. Bessonette and M. A. White, J. Chem. Phys. **110**, 3919 (1999).
[11]M. Pagliai, M. Iannuzzi, G. Cardini, M. Parrinello, and V. Schettino, ChemPhysChem **7**, 141 (2006).
[12]A. Hermann, N. W. Ashcroft, and R. Hoffmann, J. Chem. Phys. **141**, 024505 (2014).
[13]R. J. Angel, D. J. Frost, N. L. Ross, and R. Hemley, Phys. Earth Planet. Inter. **127**, 181 (2001).
[14]Q. Williams and R. J. Hemley, Annu. Rev. Earth Planet. Sci. **29**, 365 (2001).
[15]R. A. Eggleton, J. N. Boland, and A. E. Ringwood, Geochem. J. **12**, 191 (1978).
[16]D. G. Pearson, F. E. Brenker, F. Nestola, J. McNeill, L. Nasdala, M. T. Hutchison, S. Matveev, K. Mather, G. Silversmit, S. Schmitz, B. Vekemans, and L. Vincze, Nature **507**, 221 (2014).
[17]B. Schmandt, S. D. Jacobsen, T. W. Becker, Z. Liu, and K. G. Dueker, Science **344**, 1265 (2014).
[18]E. Stolper, Geochim. Cosmochim. Acta **46**, 2609 (1982).
[19]D. R. Bell and G. R. Rossman, Science **255**, 1391 (1992).
[20]R. A. Lange, Rev. Mineral. Geochem. **30**, 331 (1994), http://rimg.geoscienceworld.org/content/30/1/331.
[21]O. Fabelo, J. Pasán, L. Cañadillas Delgado, F. S. Delgado, A. Labrador, F. Lloret, M. Julve, and C. Ruiz-Pérez, CrystEngComm **10**, 1743 (2008).
[22]L.-S. Long, Y.-R. Wu, R.-B. Huang, and L.-S. Zheng, Inorg. Chem. **43**, 3798 (2004).
[23]P. S. Lakshminarayanan, E. Suresh, and P. Ghosh, Angew. Chem., Int. Ed. **45**, 3807 (2006).
[24]B. Sreenivasulu and J. J. Vittal, Angew. Chem., Int. Ed. **43**, 5769 (2004).
[25]J. Carrasco, A. Michaelides, M. Forster, S. Haq, R. Raval, and A. Hodgson, Nat. Mater. **8**, 427 (2009).
[26]L. Lin, J. A. Morrone, and R. Car, J. Stat. Phys. **145**, 365 (2011).
[27]M. Mallary, A. Torabi, and M. Benakli, IEEE Trans. Magn. **38**, 1719 (2002).
[28]Data Sheet No. DS020-EN-US-0914-01, "Ultrastar 7K6000 Hard Disk Drives" edited by Hitachi Global Storage Technologies (San Jose, CA, USA, 2014), pp. 1–2.

[29]White Paper "Blu-ray Disc Format" edited by Blu-ray Disc Association (Universal City, CA, 2012), pp. 1–42.
[30]Deuterated reagents were used to produce the sample to avoid the high neutron background scattering which is the result of the large incoherent neutron scattering cross section of the hydrogen nucleus.
[31]J. M. Besson, R. J. Nelmes, G. Hamel, J. S. Loveday, G. Weill, and S. Hull, Phys. B: Condens. Matter **180-181**, 907 (1992).
[32]R. M. Wilson, J. S. Loveday, R. J. Nelmes, S. Klotz, and W. G. Marshall, Nucl. Instrum. Methods Phys. Res., Sect. A **354**, 145 (1995).
[33]A. C. Larson and R. B. Von Dreele, General Structure Analysis System (GSAS), Technical Report 86-748, Los Alamos National Laboratory, 1994.
[34]D. C. Lonie and E. Zurek, Comput. Phys. Commun. **182**, 372 (2011).
[35]G. Kresse and J. Furthmüller, Phys. Rev. B **54**, 11169 (1996).
[36]G. Kresse, Phys. Rev. B **59**, 1758 (1999).
[37]J. P. Perdew, K. Burke, and M. Ernzerhof, Phys. Rev. Lett. **77**, 3865 (1996).
[38]G. Mills, H. Jónsson, and G. K. Schenter, Surf. Sci. **324**, 305 (1995).
[39]See supplementary material at http://dx.doi.org/10.1063/1.4938260 for crystal structure information, $p - V$ relations and Bader partial charges.
[40]H. P. Beck and G. Lederer, J. Chem. Phys. **98**, 7289 (1993).
[41]Note that in our calculations, we can not model the proton disorder seen in the room-temperature KOH-II phase.
[42]A. F. Goncharov, V. V. Struzhkin, H.-k. Mao, and R. J. Hemley, Phys. Rev. Lett. **83**, 1998 (1999).
[43]Y. Bronstein, P. Depondt, F. Finocchi, and A. M. Saitta, Phys. Rev. B **89**, 214101 (2014).
[44]J. D. Bernal and R. H. Fowler, J. Chem. Phys. **1**, 515 (1933).
[45]N. Bjerrum, Mat.-Fys. Medd. - K. Dan. Vidensk. Selsk. **27**, 1 (1951).
[46]K. Aoki, H. Yamawaki, M. Sakashita, and H. Fujihisa, Phys. Rev. B: Condens. Matter **54**, 15673 (1996).
[47]M. Benoit, A. H. Romero, and D. Marx, Phys. Rev. Lett. **89**, 145501 (2002).
[48]C. Mailhiot, L. Yang, and A. McMahan, Phys. Rev. B: Condens. Matter **46**, 14419 (1992).
[49]M. I. Eremets, A. G. Gavriliuk, I. A. Trojan, D. A. Dzivenko, and R. Boehler, Nat. Mater. **3**, 558 (2004).
[50]V. Iota, Science **283**, 1510 (1999).
[51]M. Amsler, J. Flores-Livas, L. Lehtovaara, F. Balima, S. Ghasemi, D. Machon, S. Pailhès, A. Willand, D. Caliste, S. Botti, A. San Miguel, S. Goedecker, and M. Marques, Phys. Rev. Lett. **108**, 065501 (2012).
[52]C. Pickard and R. Needs, Phys. Rev. Lett. **102**, 146401 (2009).
[53]M.-S. Miao and R. Hoffmann, Acc. Chem. Res. **47**, 1311 (2014).
[54]J. Sun, M. Martinez-Canales, D. D. Klug, C. J. Pickard, and R. J. Needs, Phys. Rev. Lett. **111**, 175502 (2013).
[55]A. Hermann, N. W. Ashcroft, and R. Hoffmann, Proc. Natl. Acad. Sci. U. S. A. **109**, 745 (2012).
[56]R. F. W. Bader, *Atoms in Molecules: A Quantum Theory* (Oxford University Press, Oxford, UK, 1994).
[57]A. Hermann and P. Schwerdtfeger, Phys. Rev. Lett. **106**, 187403 (2011).
[58]D. L. V. K. Prasad, N. W. Ashcroft, and R. Hoffmann, J. Phys. Chem. A **116**, 10027 (2012).
[59]J. P. Perdew, R. G. Parr, M. Levy, and J. L. Balduz, Phys. Rev. Lett. **49**, 1691 (1982).
[60]M. S. Hybertsen and S. G. Louie, Phys. Rev. B **34**, 5390 (1986).
[61]S. Albrecht, L. Reining, R. Del Sole, and G. Onida, Phys. Rev. Lett. **80**, 4510 (1998).
[62]P. H. Hahn, W. G. Schmidt, K. Seino, M. Preuss, F. Bechstedt, and J. Bernholc, Phys. Rev. Lett. **94**, 37404 (2005).
[63]A. Hermann, W. G. Schmidt, and P. Schwerdtfeger, Phys. Rev. Lett. **100**, 207403 (2008).
[64]C. Drechsel-Grau and D. Marx, Phys. Rev. Lett. **112**, 148302 (2014).
[65]X. Meng, J. Guo, J. Peng, J. Chen, Z. Wang, J.-R. Shi, X.-Z. Li, E.-G. Wang, and Y. Jiang, Nat. Phys. **11**, 235 (2015).
[66]S. D. Jackson, Nat. Photonics **6**, 423 (2012).
[67]Y. Yao, A. J. Hoffman, and C. F. Gmachl, Nat. Photonics **6**, 432 (2012).